First published February 25, 2006; doi:10.1152/jn.00983.2005.

Is Equilibrium Point Control Feasible for Fast Goal-Directed Single-Joint Movements?

Dinant A. Kistemaker, Arthur (Knoek) J. Van Soest, and Maarten F. Bobbert

Institute for Fundamental and Clinical Human Movement Sciences, Vrije Universiteit, Amsterdam, The Netherlands

Submitted 19 September 2005; accepted in final form 22 January 2006

Kistemaker, Dinant, Arthur (Knoek) J. Van Soest, and Maarten F. Bobbert. Is equilibrium point control feasible for fast goal-directed single-joint movements? *J Neurophysiol* 95: 2898–2912, 2006. First published February 25, 2006; doi:10.1152/jn.00983.2005. Several types of equilibrium point (EP) controllers have been proposed for the control of posture and movement. EP controllers are appealing from a computational perspective because they do not require solving the "inverse dynamic problem" (i.e., computation of the torques required to move a system along a desired trajectory). It has been argued that EP controllers are not capable of controlling fast single-joint movements. To refute this statement, several extensions have been proposed, although these have been tested using models in which only the tendon compliance, force–length–velocity relation, and mechanical interaction between tendon and contractile element were not adequately represented. In the present study, fast elbow-joint movements were measured and an attempt was made to reproduce these using a realistic musculoskeletal model of the human arm. Three types of EP controllers were evaluated: an open-loop α-controller, a closed-loop λ-controller, and a hybrid open- and closed-loop controller. For each controller we considered a continuous version and a version in which the control signals were sent out intermittently. Only the intermittent hybrid EP controller was capable of generating movements that were as fast as those of the subjects. As a result of the nonlinear muscle properties, the hybrid EP controller requires a more detailed representation of static muscle properties than generally assumed in the context of EP control. In sum, this study shows that fast single-joint movements can be realized without explicitly solving the inverse dynamics problem, but in a less straightforward manner than implied by proponents of conventional EP controllers.

INTRODUCTION

It has been widely acknowledged that the viscoelastic properties of muscles facilitate the control of posture (e.g., Milner 2002) and movement (e.g., Brown and Loeb 2000; Van Soest and Bobbert 1993). Equilibrium point (EP) controllers form an important class of control models that exploit these viscoelastic properties. In an EP controlled system, voluntary movements are generated by changing EPs. Various EP controllers have been proposed in the literature, which differ in the way EPs are defined (see McIntyre and Bizzi 1993), but have in common that there is no need to calculate the torques required to move a system along a desired trajectory by solving the "inverse dynamics problem."

Two classes of EP controllers have received a lot of attention in the literature: the α-model and the λ-model. According to the α-model (e.g., Bizzi and Abend 1983; Hogan 1984), an EP is set by defining the "rest length" and the stiffness of the muscles crossing a joint, both of which are determined by the α-motoneuron activity (McIntyre and Bizzi 1993). Although the α-model does not need information about the dynamical properties of the musculoskeletal system, it does require information about its static properties; it presupposes a representation of the relation between α-motoneuron activity and the resulting equilibrium position. Other types of EP controllers recognize that α-motoneuron activity depends not only on supraspinal input but also on low level spinal loops. For example, at a given supraspinal input, α-motoneuron activity, and consequently muscle force, depends on afference from muscle spindles. This prompted Merton (1953) to suggest that low-level spinal loops could form the basis for EP control. In his "servo"-controller, γ-motoneuron activity prescribes the desired lengths of muscle spindles, that is, the lengths that they would have if the system were in the desired EP. As long as actual spindle length deviates from the desired length, spindles produce afference that drives α-motoneuron activity, causing the system to accelerate in the direction of the EP. However, this type of control is not supported by experiments because at movement initiation α- and γ-motor units become active simultaneously (Vallbo 1970). Another EP controller, in which α-motoneuron activity depends on feedback, is the so-called λ-model (e.g., Feldman 1986). In abstract terms, the λ-model assumes that an EP can be set by defining the threshold (λ) of the stretch reflex of all muscles involved. At least in the original version, this controller needs only a representation (or "map") that relates joint angles to muscle lengths to generate control signals.

To improve the performance of EP controllers, two extensions have been proposed in the literature. First, a cocontraction command was added to increase stiffness, resulting in a faster movement toward the desired EP (e.g., Gribble et al. 1998). However, as was already argued by Gottlieb (1998b), whereas this would be straightforward to implement if the muscles in the effector system had identical invariant angle–torque characteristics, it remains to be shown whether an adequate cocontraction command can be easily generated when realistic muscle models are used. Second, velocity feedback was added to improve the damping characteristics of the system (e.g., Feldman 1986), and it has been advocated to include a contraction velocity reference signal and feed back the difference between desired and actual contraction velocity (de Lussanet et al. 2002; McIntyre and Bizzi 1993) rather than the actual velocity.

Address for reprint requests and other correspondence: D. A. Kistemaker, Institute for Fundamental and Clinical Human Movement Sciences, Vrije Universiteit, van der Boechorststraat 9, 1081 BT Amsterdam, The Netherlands (E-mail: d.kistemaker@fbw.vu.nl).

The costs of publication of this article were defrayed in part by the payment of page charges. The article must therefore be hereby marked "*advertisement*" in accordance with 18 U.S.C. Section 1734 solely to indicate this fact.

It has been argued that EP control is not feasible for fast single-joint movements (e.g., Schaal 2002; Schweighofer et al. 1998) or, alternatively, that EP controllers need complex EP trajectories to control fast single-joint movements (e.g., Bellomo and Inbar 1997; Hogan 1984; Latash and Gottlieb 1991; Popescu et al. 2003). However, both claims, as well as attempts to refute them (e.g., Gribble and Ostry; 2000; Gribble et al. 1998; St-Onge et al. 1997), were based on results of simulations with models of the musculoskeletal system in which the viscoelastic properties of muscles were inadequately represented or not at all. When testing EP controllers with musculoskeletal models, it is of paramount importance to use a realistic model of the muscles. For example, the maximally attainable movement speed depends on muscle properties such as the force–velocity relationship. It has been argued (Gribble et al. 1998; but see Nakano et al. 1999) that the complex and nonmonotonic nature of (virtual) EP trajectories derived on the basis of comparison of simulation results with experimental results (Gomi and Kawato 1996; Latash and Gottlieb 1991) was attributed to oversimplification of the force–velocity relationship of the modeled muscles. Furthermore, most EP controllers have been tested with models that ignored the series compliance of muscle; especially in pennate muscles, with relatively short muscle fibers, this series compliance may be large (the compliance resides not only in tendons, but also in aponeuroses); we will use "tendon compliance" as shorthand for the total series elasticity. In a musculoskeletal model that does not incorporate tendon compliance, EP controllers can control joint angle by setting the appropriate muscle lengths (i.e., the length of the muscle–tendon complex as a whole) using feedback from muscle spindles (e.g., Gribble et al. 1998; Latash and Gottlieb 1991). In reality, however, muscle spindle feedback is not related to muscle length but to *muscle fiber* length, and tendon compliance causes the relation between muscle fiber length and total muscle length to depend on muscle force. Furthermore, when tendon compliance is ignored, contraction velocity becomes proportional to angular velocity, which results in physiologically implausible muscle behavior (e.g., Zajac 1989).

Interestingly, both neurophysiological and behavioral studies suggest that humans control their movements intermittently. For example, during voluntary movements of the finger (Evans and Baker 2003; Valbo and Wessberg 1993), wrist (Conway et al. 2004; Kakuda et al. 1999), and elbow (Conway et al. 1997; Doeringer and Hogan 1998), humans typically show 6- to 12-Hz variations in angular velocity. Wessberg and Vallbo (1996) provided evidence that reflex responses during finger movements are too weak to account for the observed intermittent modulation of motor output. It is conceivable that motor neuron pool dynamics play a role in the observed intermittency. However, recent studies of Gross et al. (2002) and Pollok et al. (2005) indicated that finger movements are driven by a cerebello-thalamo-cortical loop with a frequency of about 8–12 Hz. These observations are complemented by a recent study of Conway et al. (2004) in which a low-frequency ($<$12 Hz) coupling was found between motor cortex EEG and muscle EMG during the execution of fast wrist movements. Combined, these findings suggest that, whereas the feedback components of muscle stimulation are sent out continuously, the open-loop components are sent out intermittently. This leads to the question to what extent this intermittency affects the EP control of fast movements.

The main purpose of this study was to investigate whether EP control using simple EP trajectories is feasible for fast single-joint arm movements. Elbow angle and EMG were measured during fast point-to-point elbow movements. Subsequently, it was attempted to reproduce the experimentally observed movements with a realistic musculoskeletal model of the arm, controlled by three types of EP controllers: an open-loop α-controller, a closed-loop λ-controller, and a hybrid open- and closed-loop EP controller. To investigate the influence of intermittent control, we also performed simulations in which the open-loop components of these EP controllers were sent out intermittently. It will be shown that all EP controllers gain movement speed when control signals are sent out intermittently rather than continuously. Furthermore, it will be shown that an intermittent version of the hybrid EP controller is capable of making the model reproduce the fast point-to-point movements observed in the subjects, from which we will conclude that EP control cannot be dismissed when considering fast point-to-point single-joint movements.

METHODS

Experimental protocol

After providing informed consent, six male participants (age 27 $\pm$ 2 yr) were seated on a nonrotating chair behind a table with their arm in a horizontal plane through both shoulders. The lower arm was strapped to a light glass fiber tube (0.48 m; 0.345 kg) that was attached to the table with a hinge. The participants were seated such that the flexion–extension axis of the elbow joint was aligned with the axis of the hinge. The shoulder angle was 45° (see Fig. 1, *A* and *B* for definitions of elbow and shoulder joint angle). Three blocks made of polystyrene were placed on the table at a distance of 60 cm from the hinge, corresponding to elbow angles of 45, 95, and 145°. A laser pointer was mounted to the end of the tube such that when the tube rotated in the horizontal plane, the laser beam hit the blocks at their centers. Participants were instructed to direct the light of a small laser pointer (13.5 g), mounted on the end of the tube, to the marked middle of one block and then, on an auditory cue, to direct it as fast as possible to the marked middle of another block. Participants performed fast point-to-point movements in six randomized conditions, each consisting of 15 trials: elbow flexion movements Flex1–3 of 100° and Flex1–2 and Flex2–3 of 50°; and extension movements Ext3–1 of 100° and Ext2–1 and Ext3–2 of 50°. Before the 15 trials in each condition, participants practiced until they could move fast to the target with minimal overshoot. Breaks of 5 min were interspersed between conditions.

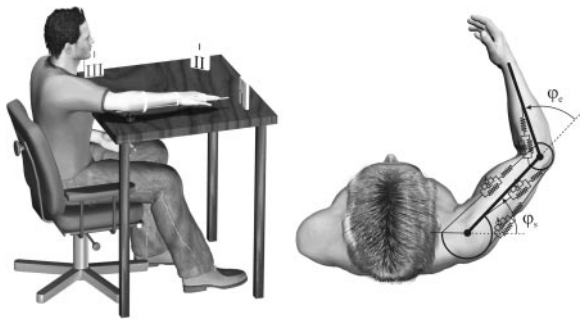

FIG. 1. Experimental setup (*A*) and musculoskeletal model (*B*).

Data collection and signal processing

Elbow angle time histories were recorded using a potentiometer (Sakae, FCP40A, sample rate 1,000 Hz) and low-pass filtered at a cutoff frequency of 20 Hz using a fourth-order zero-lag Butterworth filter. Myoelectric activity was recorded (TMS Porti, Enschede, The Netherlands, sample rate 1,000 Hz) from *m. biceps*, *m. brachoradialis*, *m. triceps caput longum*, and *m. triceps caput laterale*, using pairs of surface electrodes (Medi-trace, pallet electrodes, center-to-center electrode distance 2 cm) attached to the skin after standard skin preparation (Hermens et al. 1999). EMG signals were amplified, band-pass filtered (10–500 Hz), and full-wave rectified. For each participant, the six movements with the highest peak angular velocity per condition were selected that did not show more than 10° overshoot of the target.

Musculoskeletal model of the arm

The musculoskeletal model of the arm consisted of three segments, connected by two hinges representing the glenohumeral joint and the elbow joint, respectively (Fig. 1*B*). To reproduce the experimental data, only elbow flexion–extension movements in the horizontal plane were allowed. The lower arm was actuated by four lumped muscles: a monoarticular elbow flexor (*m. brachioradialis*, *m. brachialis*, *m. pronator teres*, *m. extensor carpi radialis*), a monoarticular elbow extensor (*m. triceps brachii caput laterale*, *m. triceps brachii caput mediale*, *m. anconeus*, *m. extensor carpi ulnaris*), a biarticular elbow flexor (*m. biceps brachii caput longum* and *caput breve*), and a biarticular elbow extensor (*m. triceps brachii caput longum*). Muscle-specific parameters (maximal isometric force, tendon slack length, optimum contractile element length, and moment arms; see APPENDIX A) were obtained from the literature (Murray et al. 1995, 2000; Nijhof and Kouwenhoven 2000). The parameter values of the lumped muscles were a weighed sum of the parameter values of their component muscles, with the weight factors depending on the contribution of each component muscle to the total moment. Nonspecific muscle parameters were taken from Van Soest and Bobbert (1993).

The muscles were modeled as Hill-type units (see APPENDIX A, Fig. A1) consisting of a contractile element (*CE*), a parallel elastic element (*PE*), and a series elastic element (*SE*). In previous research, it was shown that the implemented Hill-type muscle model is capable of reproducing the characteristic features of the dynamical behavior of muscles (e.g., Bogert et al. 1998; Winters and Stark 1985; Zajac 1989). Activation dynamics, describing the relation between the excitatory signal of the muscle and active state, was modeled according to Hatze (1981; see also Fig. 3). In line with Hatze's description, the excitatory signal of the model was termed muscle stimulation (*STIM*).

It was previously shown elsewhere that the resulting muscle model accounts for the experimentally observed length-dependent Ca^{2+} sensitivity of a muscle and the stimulation dependency of optimum length (Kistemaker 2005). The parameters used were equal for all controllers and kept constant during the simulations. A detailed description of the muscle model is provided in APPENDIX A and all parameter values are listed in Tables A1 and A2 of APPENDIX A. For relevant abbreviations, see Glossary (APPENDIX C).

In a previous study a musculoskeletal model was developed in which isometric elbow angle–torque relations agreed with those reported in a recent study (Kistemaker et al., unpublished observations). Using this model, it was found that stable open-loop EPs could be achieved over the whole range of motion of the elbow joint and stiffness (ranging from 18 to 42 Nm rad^{-1} depending on elbow-joint angle) could be controlled independently by means of cocontraction. In the present study we also tested the sensitivity of the simulation results to model parameter values determining the activation and contraction dynamics (see APPENDIX B).

A variable step-size ordinary differential equation solver based on the Runge–Kutta (4,5) formula was used to numerically solve the differential equations of the musculoskeletal model. Model and simulations were implemented in MATLAB 6.5 Release 13.

Controllers

An EP trajectory was defined as a "ramp" trajectory from the initial to the final position (see Fig. 2*A*). Based on the experimental data, desired movement time was estimated to be 0.20 s for the movements of 100° and 0.18 s for the movements of 50°. The stimulation defining an open-loop EP in the absence of external forces will from now on be referred to as $STIM_{open}$. As mentioned earlier, three different types of EP controllers were implemented: an open-loop α-controller, a closed-loop λ-controller, and a hybrid open- and closed-loop controller. The muscle stimulation generated by the α-controller was only $STIM_{open}$. The muscle stimulation generated by the λ-controller depended solely on the difference in desired (λ) and actual *CE* length (l_{CE}) and *CE* contraction velocity (v_{CE}). Feedback of l_{CE} and v_{CE} was assumed to be linear and a 25-ms time delay in the feedback loop was modeled using a fifth-order Padé approximation (Golub and Van Loan 1989). The muscle stimulation that resulted solely from feedback will from now on be referred to as $STIM_{closed}$. The muscle stimulation

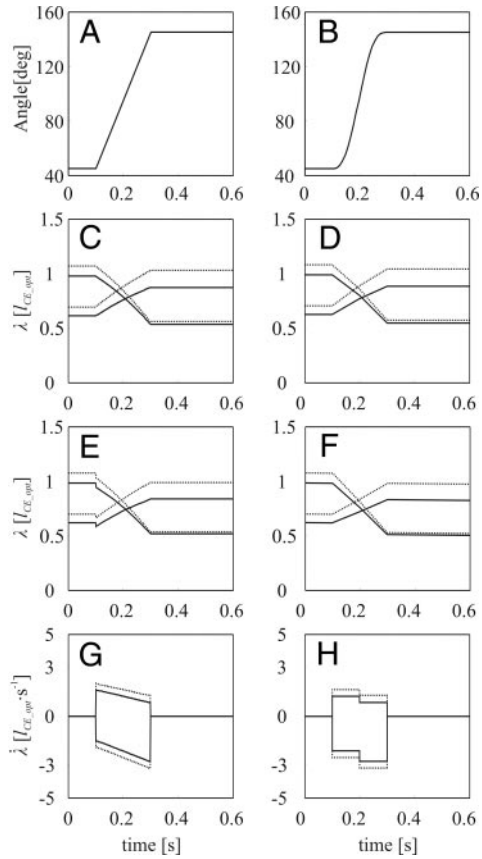

FIG. 2. *A*: ramp equilibrium point (EP) trajectory used to create control signals. *B*: minimal jerk trajectory used to optimize the feedback gains. Based on the ramp EP trajectory, desired contractile element (*CE*) length (λ) was calculated for the continuous (*C*) and intermittent (*D*) λ-controller and for the continuous (*E*) and intermittent hybrid EP controller (*F*). Continuous lines refer to the monoarticular elbow flexor and extensor; the dashed lines refer to the biarticular elbow flexor and extensor. Small dip in λ at the onset of the movement noticeable in *E* was caused by the change from lowest possible muscle stimulation ($STIM_{open}$) before movement onset to $STIM_{open}$ yielding the highest stiffness during the movement. *G* and *H*: desired *CE* contraction velocities ($\dot{\lambda}$) of the continuous and intermittent hybrid EP controllers, respectively. Note that when λ is sent out intermittently, $\dot{\lambda}$ is no longer the time derivative of λ. Traces are shown are for the condition in which participants had to flex their arm over 100° (Flex1–3).

generated by the hybrid EP controller was the sum of $STIM_{open}$ and $STIM_{closed}$. The contraction velocity feedback in this controller depended on the difference between desired ($\dot{\lambda}$) and actual v_{CE}. Figure 2 shows the λ and $\dot{\lambda}$ traces for λ- and hybrid EP controller. More details on the implementation of the controllers are provided below.

α-Controller

When the α-controller was used (see Fig. 3*A*), $STIM_{open}$ was the only input of the musculoskeletal system

$$STIM_{\alpha}(t) = STIM_{open}(t) \quad (1)$$

Not surprisingly, exploration of the model showed that the fastest movements were generated when $STIM_{open}$ was set to produce the highest low-frequency joint stiffness possible (results not shown). Because our interest was in fast movements, the *STIM* yielding the highest stiffness was selected. The only exception was $STIM_{open}$ at the equilibrium starting position, which, in line with the empirical observation that muscle activity is practically absent at initial positions (e.g., Gottlieb 1998a; Ostry and Feldman 2003; Suzuki et al. 2001), was chosen such that it minimized the sum of the individual muscle stimulations.

λ-Controller

The total muscle stimulation generated by the λ-controller ($STIM_{\lambda}$) depended on the difference between λ (activation *CE* threshold length) and l_{CE} and on v_{CE} (see Fig. 3*B*)

$$STIM_{\lambda}(t) = STIM_{closed}(t) = \{k_p[\lambda - l_{CE}(t-\delta)] + k_d[-v_{CE}(t-\delta)]\}_0^1 \quad (2)$$

where k_p and k_d are feedback constants that will be optimized (see following text) and δ (=0.025 s) is a short-latency reflex delay. In the present study it was assumed that the muscle spindles provide accurate time-delayed information about l_{CE} and v_{CE}. The expression $\{x\}_0^1$ means that values of $x > 1$ were set to 1 and negative values were set to 0.

To set an EP in terms of λ values of the muscles around the elbow joint, the relation between elbow angle and *CE* length of the individual muscles must be known. Because *SE* length depends on the force delivered by the *CE*, no one-to-one relation exists between elbow angle and *CE* lengths. This implies that a choice had to be made with respect to the mapping of *CE* to λ. In analogy to the reciprocal command (R) of the λ-model (e.g., Feldman et al. 1990), λ was chosen such that it equaled *CE* length in a desired EP with zero stimulation (see Fig. 2*B*).

Hybrid EP controller

McIntyre and Bizzi (1993) hypothesized that a combination of the α-controller and λ-controller increases movement speed. They also suggested that feedback on the difference between actual and desired velocity, instead of feedback on actual velocity alone (i.e., linear damping), would enhance the performance of the system. Both suggestions provided grounds for formulating a hybrid EP controller of the form (see Fig. 3*C*)

$$STIM_h = \{STIM_{open} + k_p[\lambda - l_{CE}(t-\delta)] + k_d[\dot{\lambda} - v_{CE}(t-\delta)]\}_0^1 \quad (3)$$

λ values were derived from the steady-state solution of the muscle model using the equilibrium angle and $STIM_{open}$. $\dot{\lambda}$ is the time derivative of λ (see Fig. 2, *E* and *G*) and k_p and k_d are feedback constants. It was assumed that the CNS is capable of generating a reference signal on basis of the desired trajectory (McIntyre and Bizzi 1993), although direct physiological evidence for this assumption is absent in the literature.

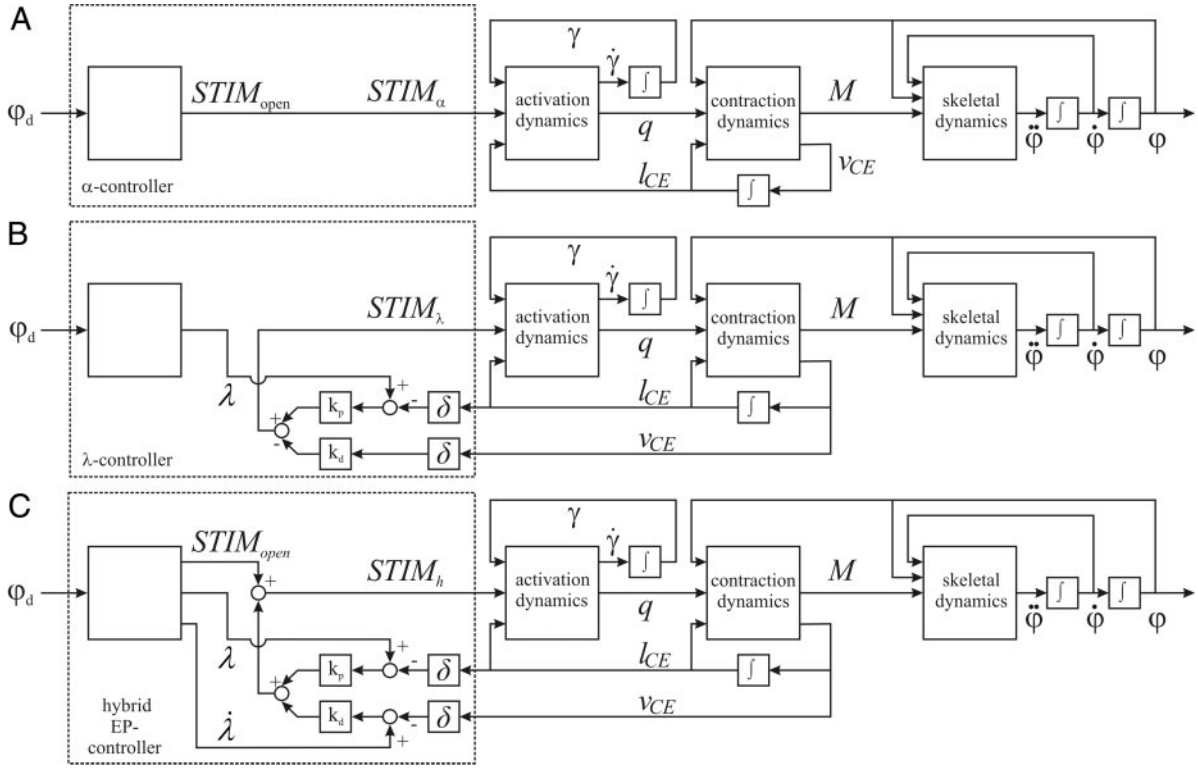

FIG. 3. Flowchart of the musculoskeletal model of the arm and the α-controller (*A*), the λ-controller (*B*), and the hybrid EP controller (*C*). Activation dynamics describes how muscle stimulation (*STIM*) leads to γ (relative amount of free Ca^{2+}), which, together with contractile element length l_{CE}, affects q (the relative amount of Ca^{2+} bound to troponin; Ebashi and Endo 1968). Contraction dynamics describes how muscle moment (M) depends on q, l_{CE}, v_{CE}, and joint angle (φ). Skeletal dynamics describes the equations of motion of the skeleton. For abbreviations see Glossary (APPENDIX C).

Intermittent controllers

Intermittent control was implemented by updating $STIM_{open}$, λ, and $\dot{\lambda}$ at a frequency of 10 Hz. Feedback was updated continuously. Note that when sending out λ and $\dot{\lambda}$ intermittently, $\dot{\lambda}$ is no longer the time derivative of λ. The algorithms defining the intermittent α-controller, λ-controller, and hybrid EP controller were the same as those for the continuous versions (see also Fig. 2).

Optimization of feedback gains

The feedback gains used for the λ-controller and the hybrid EP controller were optimized to minimize the total sum of the squared differences between simulated and desired movements for all six conditions. Thus for each controller, only one set of feedback gains was used. It is implausible that endpoint oscillations of the actual movement are part of the desired movement. Therefore for the desired movements, minimal jerk trajectories (see Fig. 2*B*) were used to optimize the feedback gains, rather than the experimental data themselves. Minimal jerk trajectories have often been used to describe the kinematics of fast point-to-point movements and do not show oscillations (e.g., Hogan 1984). The optimal values for the feedback gains were identified using a combination of a grid search and a Nelder–Mead simplex search method (Lagarias et al. 1998).

Kinematic features

To quantify the performance of the controllers, three movement features were extracted from the simulated and experimental data: peak angular velocity ($\dot{\varphi}_p$), time to peak velocity (t_{pv}), and "movement duration" (t_{mov}). t_{pv} was defined as the time between the instant that the elbow reached 5% of the total distance to be covered and the instant at which $\dot{\varphi}_p$ was reached. t_{mov} was defined as the time needed to move the arm from 5 to 95% of the total distance to be covered. Furthermore, the root-mean-squared (RMS) values were calculated between the simulated and (averaged) experimentally observed position traces. RMS values were calculated by first calculating the cross-correlation function between experimental and simulated data. Subsequently, the lag yielding the highest cross-correlation was identified. Then, the RMS value between experimental data and the simulated data, time shifted with the indicated lag, was calculated (see Table 1).

Statistical analysis

Condition-related differences in kinematic parameters were analyzed using a 2 (Direction) × 3 (Trajectory) repeated-measures ANOVA. The factor Direction had levels flexion and extension and the factor Trajectory had levels 45–145, 45–95, and 95–145° (and vice versa). Single-sample *t*-tests ($\alpha = 0.05$) were used to test for differences between the features of the simulated and experimental data.

RESULTS

Column I of Fig. 4 and *columns I* and *III* of Fig. 5 show the recorded elbow angle, angular velocity, and EMG traces for six trials of one representative participant in all six conditions. Before comparing simulation results with experimental data, it is useful to summarize the results of a statistical analysis of the experimental results. For peak angular velocity, a significant main effect of Trajectory [$F(1,5) = 246.4$; $P < 0.001$] and a significant Direction × Trajectory interaction [$F(2,10) = 5.38$; $P = 0.026$] were found. For time to peak angular velocity, we found a significant main effect of Direction [$F(1,5) = 10.15$; $P = 0.024$], a main effect of Trajectory [$F(1,5) = 68.4$; $P < 0.001$], and a significant Direction × Trajectory interaction [$F(2,10) = 7.56$; $P = 0.010$]. For movement duration we also found a significant main effect of Trajectory [$F(1,5) = 154.2$; $P < 0.001$] and a significant Direction × Trajectory interaction [$F(2,10) = 4.46$; $P = 0.041$]. Post hoc *t*-test revealed that each of the dependent variables reached different values in the large-amplitude condition (movements of 100°) than in the two small-amplitude conditions (movements of 50°), whereas the values reached in the small-amplitude conditions were not statistically different. In the large-amplitude condition higher peak angular velocities were reached than in the small-amplitude movements (mean 930 vs. 655°/s), the subjects took longer to arrive at peak velocity (mean 0.074 vs. 0.052 s), and total movement duration was greater (mean 0.128 vs. 0.093 s). For time to peak velocity, the main effect of Direction resulted from a significantly longer time to arrive at peak angular velocity in the flexion condition. The significant Direction × Trajectory interaction was the result of significant differences for peak angular velocity ($t = 3.33$; $P = 0.021$) and movement duration ($t = -3.62$; $P = 0.015$) between the Flex1–3 and Ext3–1 conditions: in the Flex1–3 condition higher peak angular velocities were reached (mean 975 vs. 886°/s) and movement duration was shorter (mean = 0.118 vs. 0.137 s) than in the Ext3–1 condition. For time to peak velocity, the significant Direction × Trajectory interaction was the result of significant differences between the small-amplitude movements. Peak angular velocity and movement duration did not differ significantly between the small-amplitude conditions, but movement duration was significantly smaller in the Ext2–1 condition than in all other movements of 50°.

Column II of Fig. 4 shows the time histories of kinematic data and *STIM* of the α-controller for conditions Flex1–3 (Fig. 4*A*) and Ext3–1 (Fig. 4*B*). Single-sample *t*-test showed that all kinematic features produced by the simulations with the continuous and intermittent α-controller were significantly different ($P < 0.01$) from those subtracted from the experimental data (see Table 2). When EPs were set intermittently, the model reacted less sluggishly and movement speed increased, but insufficiently so to match human performance. The overall resemblance between simulated movement using the α-controller and experimental data was poor, as indicated by the high RMS values (on average 37.7 and 22.5° for the continuous and intermittent version, respectively; see Table 2).

The movements produced with the λ-controller (*column III* of Fig. 4) also failed to match experimental data: all kinematic features were significantly different ($P < 0.001$) from those observed experimentally. Apart from reaching a significantly lower peak angular velocity (see Table 2) and taking more time, the model exhibited marked endpoint oscillations. The relatively high feedback gains, necessary to minimize the error between the actual trajectory and the minimal jerk trajectory, were the main cause of these oscillations. When additional

TABLE 1. *Kinematic features of experimental results*

Condition	$\dot{\varphi}_p$, [deg s^{-1}]	t_{pv}, [s]	t_{mov}, [s]
Flex1–3	975	0.077	0.118
Flex1–2	628	0.062	0.104
Flex2–3	633	0.057	0.092
Ext3–1	−848	0.072	0.137
Ext2–1	−668	0.051	0.089
Ext3–2	−688	0.057	0.085

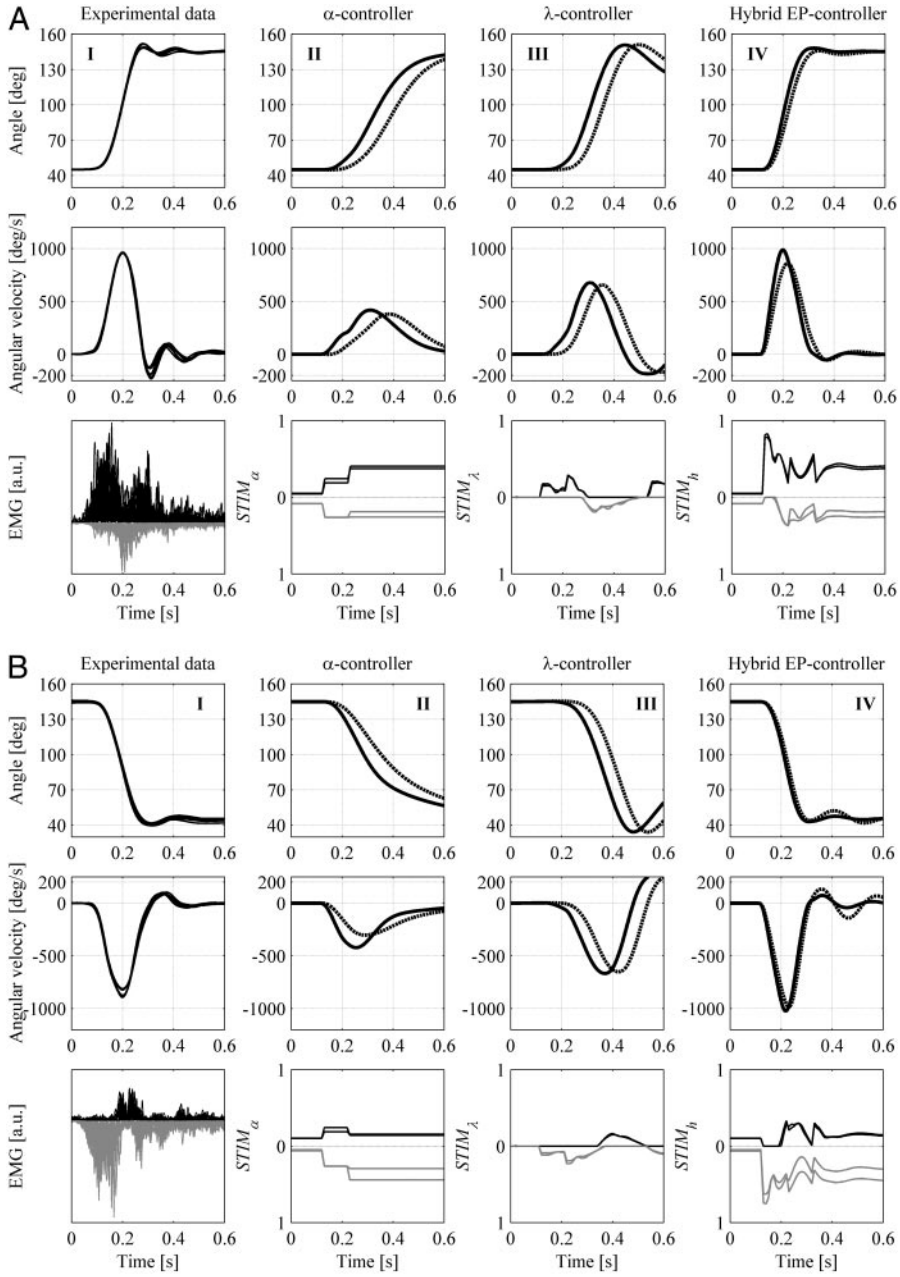

FIG. 4. Overview of experimental data and simulation results. *Column I*: elbow angle, angular velocity, and EMG measured in conditions Flex1–3 (*A*) and Ext3–1 (*B*). *Columns II*, *III*, and *IV*: outcome of simulations of the musculoskeletal model controlled by the α-, λ-, and hybrid EP controllers, respectively. Continuous lines refer to intermittent control, dashed lines to continuous control. *Top EMG/STIM traces* refer to the 2 elbow flexors, *bottom traces* to the 2 elbow extensors.

"penalties" on endpoint oscillations were introduced in the optimization criterion, feedback gains and oscillations decreased, but at the cost of movement speed (results not shown). As with the α-controller, the RMS values were high (on average 23.5 and 17.9° for the continuous and intermittent version of the λ-controller, respectively), indicating a poor resemblance between simulated and experimentally observed movements.

In both Fig. 4 and Fig. 5, *Column IV* shows the simulation obtained with the hybrid EP controller for all six conditions. This hybrid EP controller was the only controller capable of producing movements at least as fast as those observed experimentally (see Tables 2 and 3 for complete results of statistical comparison). In only one of six conditions (Ext3–2) was peak $\dot{\varphi}_p$ in the simulation significantly lower than that observed experimentally. Similarly, in only one of six conditions, the duration of the simulated movement was significantly longer than that observed experimentally (Flex2–3). Finally, peak velocity in the simulated movements was never reached later than in the experimental movements. In fact, t_{pv} was significantly smaller in the simulations in five of six conditions. The close resemblance between movements generated using the intermittent hybrid EP controller and those observed experimentally is reflected by the average RMS value, which was found to be only 2.3° (vs. 3.9° for the continuous EP controller; Table 2). In sum, the intermittent hybrid EP controller was capable of generating point-to-point movements at least as fast as those observed experimentally.

The muscle stimulation patterns generated with the hybrid EP controller were qualitatively similar to the experimentally observed EMG patterns (Figs. 4 and 5). The controller produced the triphasic burst pattern typical of fast point-to-point

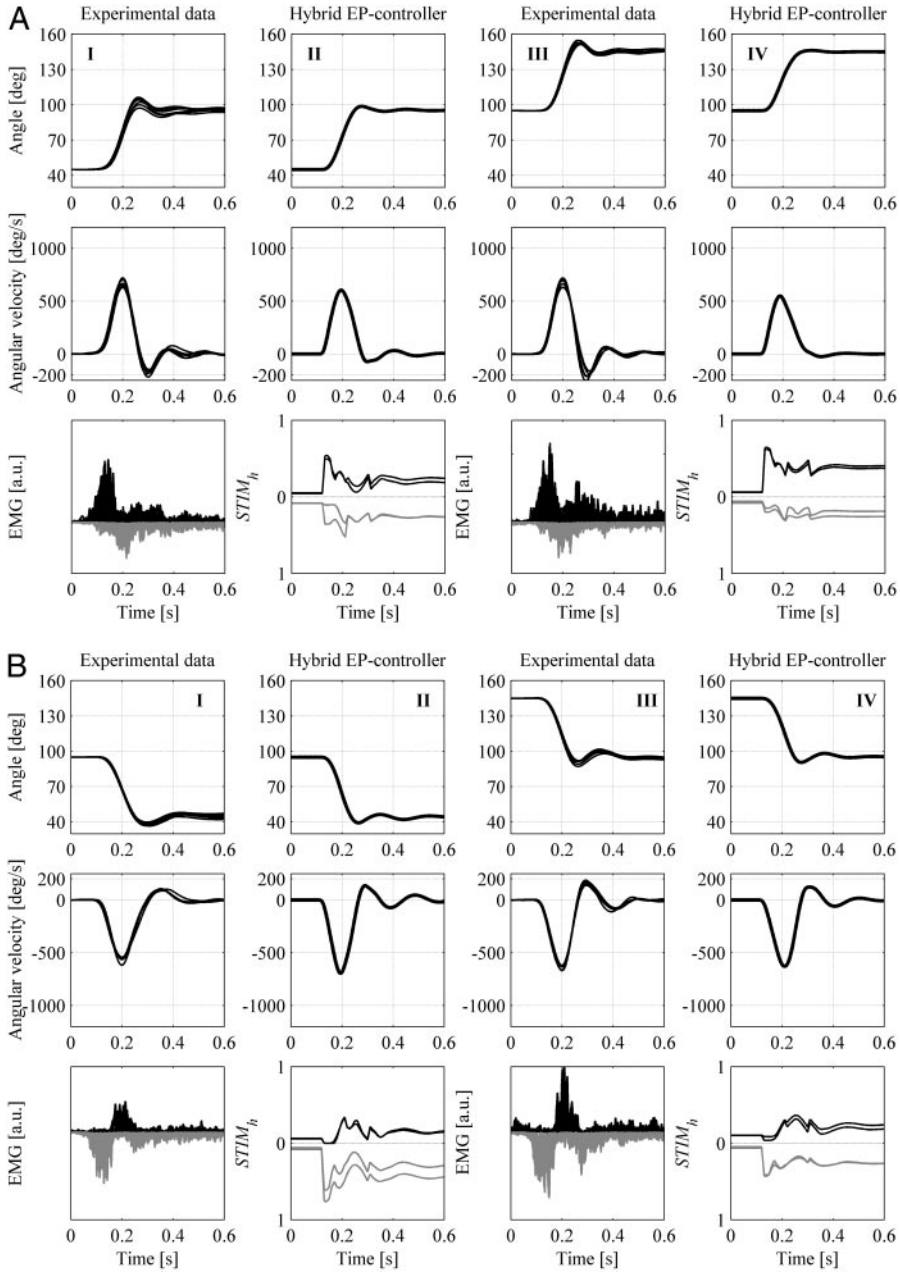

FIG. 5. Experimental data (*columns I* and *III*) and simulation results obtained with the intermittent hybrid EP controller (*columns II* and *IV*) for conditions Flex1–2 and Flex2–3 (*A*) and for conditions Ext2–1 and Ext3–2 (*B*). *Top EMG/STIM traces* refer to the 2 elbow flexors, *bottom traces* to the 2 elbow extensors.

movements (e.g., Prodoehl et al. 2003; Wachholder and Altenburger 1926; Yamazaki et al. 1993; see also Fig. 4). It can be seen in Fig. 6, which presents the separate contributions of open-loop and feedback components to the total muscle stimulation of the hybrid EP controller, that the triphasic patterns mainly originated from the contraction velocity feedback (see also Bullock and Grossberg 1992). It is still debated whether triphasic EMG bursts result predominantly from central or peripheral processes (e.g., Prodoehl et al. 2003). In line with the position of Bullock and Grossberg (1992), the results obtained in this study with the hybrid EP controller suggest that triphasic bursts need not be preprogrammed.

TABLE 2. *Kinematic features of simulation results*

Condition	$\dot{\varphi}_p$, [deg s^{-1}]			t_{pv}, [s]			t_{mov}, [s]			RMS, [deg]		
Continuous	α	λ	Hyb	α	λ	Hyb	α	λ	Hyb	α	λ	Hyb
Flex1–3	380	655	859	0.88	0.094	0.059	0.323	0.172	0.140	40.8	26.7	3.6
Ext3–1	−302	−650	−982	0.078	0.120	0.071	0.430	0.178	0.121	34.6	40.3	4.1
Intermittent	α	λ	Hyb	α	λ	Hyb	α	λ	Hyb	α	λ	Hyb
Flex1–3	417	688	987*	0.119	0.109	0.052	0.323	0.181	0.118*	24.0	11.4	2.5
Ext3–1	−421	−676	−1018	0.068	0.122	0.060	0.389	0.175	0.111	21.0	24.4	2.4

Kinematic features indicated by * are not significantly different from those observed in the experimental results.

TABLE 3. *Kinematic features of intermittent hybrid EP controller*

Condition	$\dot{\varphi}_p$, [deg s^{-1}]	t_{pv}, [s]	t_{mov}, [s]	RMS, [deg]
Flex1–3	987*	0.052	0.120*	2.5
Flex1–2	601*	0.043	0.090*	2.0
Flex2–3	547*	0.042	0.110	3.3
Ext3–1	−1,018	0.060	0.111	2.4
Ext2–1	−689*	0.044	0.079	2.9
Ext3–2	−628	0.057*	0.083*	0.9

DISCUSSION

The purpose of this study was to examine whether EP control is feasible for fast goal-directed single-joint movements. In an attempt to reproduce the experimentally observed fast movements, a realistic model of the human arm was used that was controlled by several types of EP controllers. All controllers generated faster movements when the control signals were sent out intermittently. However, movements as fast as those produced by the subjects could be generated by the musculoskeletal model only when the intermittent hybrid EP controller was used.

The speeds generated by the α-controller strongly depended on the local stiffness of the EP that was set. The stiffness in an EP can be seen as the change in steady-state net torque for a given deviation from that EP. Even though $STIM_{open}$ was chosen such that it maximized joint stiffness, and even though in a previous study it was shown that the maximal stiffness of the model was in agreement with the literature (Kistemaker et al., unpublished observations), maximal movement speed was insufficient to match the experimental data. By sending out the control signals intermittently rather than continuously, deviations of the current position from the (intermittent) target were initially larger, so that greater forces were produced, resulting in faster movements (see Fig. 4). The requirement that at least start and endpoint be set resulted in a minimal modulation frequency of 5 Hz. Movement speed increased when this frequency was used, but stayed well below actually observed speeds.

The λ-controller was also incapable of generating movements fast enough to match experimental data. This was mainly attributed to the fact that muscle stimulation resulted from feedback only, whereas feedback gains had to be limited to prevent time-lag–related instability and oscillatory behavior. A shorter time lag diminished this effect, but a time lag $<$25 ms used in this study is physiologically unrealistic (e.g., Funase and Miles 1999). Implementing a reference contraction velocity and intermittency in the λ-controller enhanced maximal movement speed, but the resulting movement was still not fast enough to match experimental data and, moreover, did not eliminate the oscillations shown in Fig. 4. Other studies (Gribble et al. 1998; St-Onge et al. 1997) used a duration of the EP trajectory that was half that of the intended movement. Additional simulations with the present model indeed showed that the λ-controller reacted less sluggishly and gained movement speed when the duration of the EP trajectory was halved. However, again, the resulting movement speed stayed well below that observed experimentally and, as a result of the increased velocity, the endpoint oscillations increased in amplitude. Even when both options (i.e., halved duration of EP trajectory and reference feedback) were implemented, the λ-controller was still incapable of reproducing the experimental data (see APPENDIX B).

Although substantially faster than the movements controlled by both the (intermittent) α- and λ-controller, the movements controlled by the continuous version of the hybrid EP controller were not fast enough to match the experimental data. Maximal movement speed could be increased to about the experimentally observed value by raising the feedback gains, but only at the cost of a large overshoot of the target (results not shown). However, when the control signals of the hybrid EP controller were sent out intermittently, the musculoskeletal model produced movements that were in general as fast as or faster than the fast point-to-point movements observed in our experiments. Additional simulations (APPENDIX B) further showed that the reference velocity adopted in the hybrid EP controller was indispensable to achieve a close match between simulated and experimentally observed results. As an aside we note that, given the main question of this study, it was not attempted to maximize the fit between experiment and simulation. Several possibilities exist to further improve this fit, for example by condition-specific manipulation of the duration of the EP trajectory or by allowing different feedback gains for the different muscles. Similarly, the unrealistically high levels of cocontraction near movement completion could easily be reduced by lowering the level of cocontraction (lowering $STIM_{open}$) near the end of the movement (see APPENDIX B).

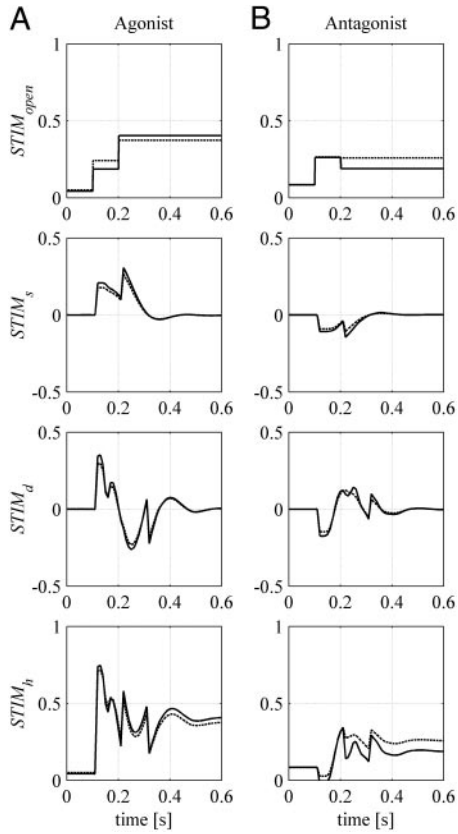

FIG. 6. Contribution of $STIM_{open}$, feedback of l_{CE} ($STIM_s$) and feedback of v_{CE} ($STIM_d$) to the total muscle stimulation of agonists (*column A*) and antagonists (*column B*) generated by the intermittent hybrid EP controller ($STIM_h$) for the Flex1–3 condition. Continuous lines refer to the monoarticular elbow flexor and extensor, dashed lines refer to the biarticular elbow flexor and extensor.

Some studies used a duration of the EP trajectory that was half the intended duration (Ghafouri and Feldman 2001; St-Onge et al. 1997). The performance of the continuous hybrid EP controller improved when such an EP trajectory was used, but its performance was worse than that of the intermittent EP controller (see APPENDIX B). The model reacted slightly faster, but was incapable of keeping up with this much faster (1,000 instead of 500°/s) EP trajectory. As a consequence, damping arising from feedback started to counteract the movement at the instant the EP trajectory reached the endpoint because from this instant onward the reference velocity equaled zero. Although an experimental study indicated that the shifts in EP during fast point-to-point movements may end approximately near peak velocity (Ghafouri and Feldman 2001), it does not seem directly beneficial for the control of fast movements when the difference between desired and actual velocity is fed back.

The hybrid EP controller, which combined open- and closed-loop components, was not simply a combination of the implemented α-controller and λ-controller. This is because the desired *CE* length (λ) depends on the total muscle stimulation (recall that, because of tendon compliance, steady-state *CE* length at a given joint angle depends on stimulation). In other words, the λ values set by the λ-controller are not equal to the *CE* lengths in a desired EP defined by the $STIM_{open}$ of the α-controller. The hybrid EP controller requires an internal representation of the following static properties of the musculoskeletal system: *1*) a map relating desired EP to $STIM_{open}$, *2*) a map relating $STIM_{open}$ to joint stiffness, and *3*) a map relating $STIM_{open}$ to steady-state *CE* length. (In essence, the implemented α-controller uses the first two maps.) Thus as a result of the complexity of the musculoskeletal model, the hybrid EP model requires a more detailed representation of static properties of the musculoskeletal system than generally used in the context of EP controllers (e.g., Gribble et al. 1998; Latash and Gottlieb 1991; McIntyre and Bizzi 1993). The feedback parameters were optimized to minimize the error between actual and desired movement and, consequently, were implicitly tuned to the parameters determining the dynamics of the musculoskeletal system. Additional simulations showed that the performance of the hybrid EP controller model was not noticeably affected when the inertial parameters of the musculoskeletal model were changed by 10% without reoptimizing the feedback gains (see APPENDIX B). This result suggests that for single-joint movements, EP control is not critically dependent on representation of dynamical parameters of the musculoskeletal system. To conclude, the present study showed that fast single-joint movements of a realistic musculoskeletal model can be adequately controlled without the requirement of solving the "inverse dynamics problem" and without an internal representation of the dynamical properties of the musculoskeletal system, albeit in a less straightforward manner than implied by most proponents of conventional EP controllers.

A major difference between the λ-controller presented in this study and most λ-models presented in the literature is that our λ-controller lacked a cocontraction or coactivation (C) command: a "simple" command that shifts all λ values to a shorter length (Feldman 1986). Because of the nonlinear behavior of the musculoskeletal system, such a simple C-command could not be derived for the present musculoskeletal model without affecting the equilibrium position (see also Gottlieb 1998b; Windhorst 1994, 1995). However, using the internal representation of the static properties that was required for the hybrid EP controller, cocontraction can be added to the λ-controller without affecting the equilibrium position. In fact, it can be shown that such a λ-controller is mathematically equivalent to the hybrid EP controller. Basically, we need to use the same three maps as those used for the hybrid EP controller, but "replace" $STIM_{open}$ by a cocontraction command (note that this cocontraction command is specific for each muscle involved). As a result of tendon compliance, the steady-state *CE* lengths in an EP can match the λ values (in terms of CE lengths) only if the controller is generating exactly the appropriate muscle stimulation at the EP: this may be accomplished by $STIM_{open}$ in the case of the hybrid EP controller and by a cocontraction command in the case of the λ-controller (note that at the EP, cocontraction is the only "source" of muscle stimulation). Once a desired EP with a desired stiffness is selected, it can easily be deduced that the cocontraction command (λ^*) for each individual muscle *must* equal

$$\lambda^* = \frac{STIM_{open}}{k_p}$$

This also shows that λ^* is in essence an open-loop component: the cocontraction command is the open-loop muscle stimulation defined in terms of *CE* length. Because steady-state *CE* length is completely determined by the cocontraction command no insight is gained by referring to the set of λ values as the "position" command (note again that, because of tendon compliance, λ does not relate one to one with joint angle). By substituting λ by ($\lambda + \lambda^*$) in *Eq. 2*, it can be seen that the modified λ-controller is mathematically equivalent to the hybrid EP controller. Therefore it can be concluded that when an appropriate cocontraction command is added to the (intermittent) λ-controller, using the representation of the static properties of the musculoskeletal system mentioned before (e.g., represented in maps), the controller is capable of generating fast point-to-point movements that resemble experimental movements. Interestingly, Feldman et al. (1990) acknowledged the need for maps relating the number of active motoneurons and their firing rates to control variables and kinematic variables; the present study provides a more detailed description of the variables that need to be coded in such maps.

When the EP controllers sent out their control signals in an intermittent rather than continuous fashion, the movements were faster and corresponded better with experimentally observed data (see Fig. 4 and Table 2). Although several studies provided evidence that humans control their movements intermittently rather than continuously (e.g., Craik 1947; Gross et al. 2002; Vallbo and Wesberg 1993; Wessberg and Vallbo 1996), intermittent control at first sight appears to be irreconcilable with the experimental results reported by Bizzi et al. (1984). Based on experiments with deafferented monkeys, Bizzi et al. (1984) showed that the final position is not set immediately at movement onset and proposed a gradual evolution of EPs. In the experiments in question, monkeys were trained to move their invisible arm to a target position. During some trials, a servo-motor was used to move the monkey's arm unnoticed from the initial position to the target position. Because the monkeys were encouraged to move their arm to this very position one would expect the arm to stay put, but

instead, when released, it started to move back in the direction of initial position. This result militates against a control scheme in which the endpoint is immediately set at movement onset. Using an estimation of movement time and distance from Fig. 6 in Bizzi et al. (1984), the intermittent versions of our controllers would generate an EP trajectory in steps of 6°. Thus the intermittent versions of the α-, λ- (if extended with the cocontraction command), and hybrid EP controllers would be capable, at least qualitatively, of reproducing Bizzi's data. Furthermore, as suggested by Bizzi and colleagues (1984), it is conceivable that for very fast movements, as studied here, the shifts in EP are more abrupt. Taken together, intermittent control as implemented in the current study does not contradict the results of experimental studies on trajectory formation during arm movement such as those reported by Bizzi et al. (1984).

A consequence of sending out control signals intermittently is that the EP trajectory is no longer identical to the desired trajectory. Other studies also suggested that EP trajectories other than the desired trajectories, such as N-shaped EP trajectories (Hogan 1984; Latash and Gottlieb 1991), underlie (and improve) the control of fast movements. However, the intermittent EP trajectory used in the present study has two advantages over N-shaped EP trajectories: *1*) as argued in the INTRODUCTION, it has both a neurophysiological and a behavioral foundation; and *2*) although the total trajectory may be different from the desired trajectory, the set points themselves are part of the desired trajectory and therefore do not require additional calculations. In the literature, the existence of intermittent behavior is often seen as an "imperfection" of the structure and functioning of the CNS (e.g., Craig 1947; Hanneton et al. 1997; Miall et al. 1993). Our results, however, suggest that intermittent control is functional in the control of fast point-to-point movements.

In this study we have assumed that the feedback gains did not vary during the movement. Although to our knowledge all studies on EP control have used continuous feedback, several studies suggest that the short-latency reflex contributions to stimulation of muscles are significantly lowered at movement onset and termination (e.g., Shapiro et al. 2002, 2004). Because this could militate against the feasibility of an EP controller (Shapiro et al. 2004), we performed additional simulations in which the contribution of feedback was gated using a Gaussian function such that feedback was absent at the beginning and end of the movement (the gating of feedback did not interact with the open-loop muscle stimulation, as may be noted from *Eq. B1* in APPENDIX B). It was found that the hybrid EP controller suffered no performance loss when feedback was gated (see APPENDIX B); the lack of feedback at the beginning of the movement was compensated by the much higher (optimized) feedback gains. Because feedback is absent at the beginning and end of the movement, the high feedback gains used did not result in instability or oscillatory behavior. Thus the hybrid EP controller is still capable of controlling fast single-joint movements when feedback is diminished at movement on- and offset.

All in all, the results of this study refute the claim that EP controllers cannot account for fast single-joint movements (e.g., Schaal 2002; Schweighofer et al. 1998), as well as the claim that EP controllers need complex EP trajectories to control fast single-joint movements (e.g., Bellomo and Inbar 1997; Hogan 1984; Latash and Gottlieb 1991; Popescu et al. 2003). However, they do not refute the claim that EP controllers predict high stiffness during fast single-joint movements (e.g., Gomi and Kawato 1997; Popescu et al. 2003). Given the intricacies of experimental determination of stiffness, we would suggest addressing this issue by comparing experimentally estimated stiffness to that predicted by the EP controlled model when subjected to the same perturbation. This remains a challenge for further research.

Although we showed that EP control is feasible in the context of fast point-to-point single-joint movements in the absence of external forces, the question remains whether the present results are generalizable to the control of movements under various circumstances involving, for example, multijoint movements and gravity. The presented hybrid EP controller is presumably able to generate control signals for multijoint movements, provided that the maps mentioned earlier are expanded for all joints and muscles involved. However, the resemblance between experimental and simulated data of single-joint movements does not guarantee that simulated multijoint movements will match experimental data as well. An important difference between single- and multijoint systems is that, in the latter, stiffness is no longer a single-valued function of $STIM_{open}$. This implies that nontrivial assumptions have to be made to select $STIM_{open}$. Also, it has been shown that "interaction torques" (i.e., torques that arise at one joint as a result of movements at the other) are taken into account by the CNS, which would be inconsistent with EP control (but see Gribble and Ostry 2000). Furthermore, it has been suggested in the literature that mono- and biarticular muscles have distinct roles during movement (Hof 2001; Van Ingen Schenau 1987), a proposition not taken into account by EP controllers, at least not explicitly.

In this study, the arm was restricted to move in a horizontal plane, so that the movement was not affected by gravity. When the arm is moved outside the horizontal plane, static errors between desired EP and actual position will occur, unless gravity on the arm and on loads possibly carried by the hand is accounted for in the maps used by the EP controller. Errors (or their compensations) will depend on the exact orientation of the arm in the gravitational field, its static properties, and the stiffness induced by both muscles and feedback. When the upper arm of the model was placed vertically and the lower arm horizontally (thereby maximizing the influence of gravity), the deviation from the desired EP was $<2°$ if $STIM_{open}$ was set such that open-loop stiffness was maximal (in this case about 20 Nm rad^{-1}), and about 5° with the lowest possible amount of cocontraction. When external loads on the hands are considered, however, the deviation from the desired position soon became unacceptably large. Thus in our view, external forces such as gravity should be taken into account by the controller.

In sum, although this study has demonstrated that EP control cannot be dismissed when considering fast point-to-point single-joint movements, it remains to be established whether EP control is feasible when multijoint movements in the presence of external forces are considered.

APPENDIX A

The implemented Hill-type muscle model consists of a contractile element (*CE*), a series elastic element (*SE*), and a parallel elastic element (*PE*) as shown schematically in Fig. A1. The mechanical behavior of the muscle is described by two coupled first-order differential equations. One first-order dynamical system describes the activation dynamics and related the muscle stimulation (*STIM*) to active state (q). The other first-order dynamical system describes the relation between the contraction velocity (v_{CE}) and the length of the contractile element (l_{CE}), depending on q, the force–length–velocity relationship of *CE*, and the passive forces of *SE* and *PE*. The length of the muscle–tendon complex (l_{MTC}) and moment arm (*arm*) are functions of joint angle. A detailed description of the muscle model is provided below (see also the flowchart of the model presented in Fig. 3; see Glossary in APPENDIX C for the relevant abbreviations).

Activation dynamics

Activation dynamics was modeled according to Hatze (1981; see also Kistemaker et al. 2005) and related muscle stimulation (*STIM*) to active state (q) in two steps. A first-order dynamical system related the free Ca^{2+} concentration (relative to its maximum value; γ_{rel}) to *STIM*. Subsequently, an algebraic relation described how active state q depends on γ_{rel} and (by ρ) on *CE* length relative to its optimum (l_{CE_rel})

$$\dot{\gamma}_{rel} = m(STIM - \gamma_{rel}) \tag{A1}$$

$$q = \frac{q_0 + (\rho\gamma_{rel})^3}{1 + (\rho\gamma_{rel})^3} \tag{A2}$$

with ρ a function of l_{CE_rel}

$$\rho = c\,\eta\,\frac{(k-1)}{(k - l_{CE\_rel})} l_{CE\_rel} \tag{A3}$$

where η, k, c, m, and q_0 are constants (see Table A1).

The original equations of Hatze are slightly simplified for clarity. For a graphical representation of the *STIM*–q relationship as a function of l_{CE_rel}, see Fig. A2*C*.

Contraction dynamics

Contraction dynamics was modeled by relating the contraction velocity (v_{CE}) to l_{CE}

$$v_{CE} = f(l_{CE}, q, \varphi) \tag{A4}$$

The contraction velocity was derived from the difference between the isometric force (F_{isom}), calculated using the force–length relationship, and the actual force to be generated by the *CE* (F_{CE}). Assuming that the mass of the muscle was negligible with respect to the force it is producing, F_{CE} equaled the difference between the force of *SE* (F_{SE}) and that of *PE* (F_{PE}). The concentric ($v_{CE} < 0$ or $F_{CE} < F_{isom}$) and eccentric ($v_{CE} > 0$ or $F_{CE} > F_{isom}$) parts of the force–velocity relationship were modeled separately. The concentric part was described based on the classic Hill equation, which was solved for v_{CE_rel} (the time derivative of l_{CE_rel})

$$v_{CE\_rel} = \frac{b^*_{rel}(F_{CE\_rel} - qF_{isom\_n})}{F_{CE\_rel} + qa^*_{rel}} \tag{A5}$$

with F_{CE_rel} ($=F_{CE}/F_{MAX}$) and F_{isom_n} ($=F_{isom}/F_{MAX}$). Based on experimental results (Stern 1974), maximal contraction velocity was made dependent on F_{isom_n} by setting: $a^*_{rel} = a_{rel}F_{isom\_n}$ when $l_{CE} > l_{CE\_opt}$ and $a^*_{rel} = a_{rel}$ when $l_{CE} \leq l_{CE\_opt}$. Furthermore, based on experimental results of Pertrofsky and Philips (1981), for low values of q, maximal contraction velocity was made dependent on q by setting

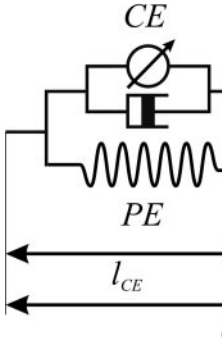

FIG. A1. Schematic representation of the Hill-type muscle model used in this study. For abbreviations see Glossary (APPENDIX C).

TABLE A1. *Muscle nonspecific parameters*

m	11.30	*width*	0.66
c	1.37e-4	a_{rel}	0.41
η	5.27e4	b_{rel}	5.20
q_0	5.00e-3	q_{crit}	0.03
k	2.90		

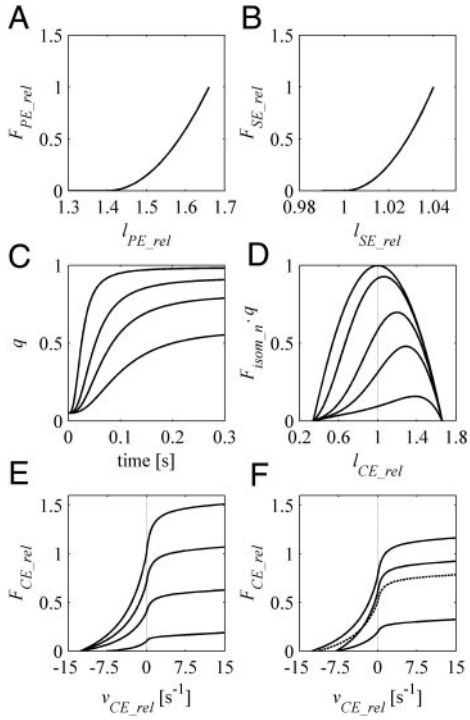

FIG. A2. *A*: force–length relationship for parallel elastic element (*PE*): $l_{PE\_rel} = l_{PE}/l_{CE\_0}$. *B*: force–length relationship of series elastic element (*SE*): $l_{SE\_rel} = l_{SE}/l_{SE\_0}$. *C*: $q(t)$ for *STIM* = 0.3 and l_{CE_rel} = 0.6, 0.8, 1.0, 1.4 (longer l_{CE_rel} = higher q). *D*: isometric force–length relationship for *STIM* = 0.05, 0.1, 0.15, 0.3, 1.0 (higher *STIM* = higher force). *E*: force–velocity relationship for l_{CE_rel} = 1.0 and q = 0.1, 0.4, 0.7, 1.0 (higher q = higher F_{CE_rel}). Note that for q <0.3, maximal shortening velocity scales with q. *F*: force–velocity relationship for *STIM* = 0.2 and l_{CE_rel} = 1.0, 1.4, 0.8 (dashed), 0.6 (in order of highest maximal F_{CE_rel}). Note that for l_{CE_rel} >1, maximal shortening velocity scales with F_{isom_n}. Maximal shortening velocity of the lower force–velocity relationship in *F* is diminished because at this *STIM* and l_{CE_rel}, q is <0.3 (see *E*).

$$b^*_{rel} = b_{rel}\left[1 - 0.9\left(\frac{q - q_{crit}}{q_0 - q_{crit}}\right)\right]^2 \quad (A6)$$

when $q < q_{crit}$ and $b^*_{rel} = b_{rel}$ when $q \geq q_{crit}$. The values for the constants a_{rel}, b_{rel}, and q_{crit} are given in Table A1.

The eccentric part of the force–velocity relationship was modeled using a hyperbola. To prevent numerical problems, a hyperbola with a slightly slanted asymptote was used (for the sake of conciseness, it was not solved here for v_{CE_rel})

$$(F_{CE\_rel} + p_3 + p_4 v_{CE\_rel})(v_{CE\_rel} + p_1) = p_2 \quad (A7)$$

The parameters p_1, p_2, p_3, and p_4 were calculated using four criteria: *1*) the concentric and eccentric curve are continuous; *2*) based on Katz (1939), the derivative of F_{CE_rel} with respect to v_{CE_rel} at $v_{CE\_rel} = 0$ of the eccentric curve was twice that of the concentric curve; *3*) the asymptote had a value of $1.5qF_{isom\_n}$ at $v_{CE\_rel} = 0$; and *4*) an arbitrary small value for the slope of the asymptote. Note that the calculated parameters were functions of F_{isom_n} such that both parts of the force–velocity relationship depended on F_{isom_n} and F_{CE_rel}. See Fig. A2, *E* and *F* for a graphical representation of the force–velocity relationship at different values of q and l_{CE_rel}.

Normalized isometric force (F_{isom_n}) was modeled as a second-order polynomial with an optimum at $l_{CE\_rel} = 1$ and two zero-crossings at $l_{CE\_rel} = 1 \pm width$

$$F_{isom\_n} = -al^2_{CE\_rel} + 2al_{CE\_rel} - a + 1 \quad (A8)$$

with $a = 1/width^2$. For a graphical representation of the isometric force–length–stimulation relation, see Fig. A2*D*.

The passive force–length characteristic of the *PE* was modeled to depend quadratically on l_{CE_rel} (note that $l_{PE} = l_{CE}$)

$$F_{PE} = k_{PE}\left[\max\left(0, l_{CE\_rel} - \frac{l_{PE\_0}}{l_{CE\_opt}}\right)\right]^2 \quad (A9)$$

$l_{PE\_0} = 1.4l_{CE\_opt}$ and k_{PE} was chosen such that $F_{PE} = 0.5F_{MAX}$ at $l_{CE\_rel} = 1 + width$. The passive force characteristic of the *SE* was modeled to depend quadratically on l_{SE}

$$F_{SE} = k_{SE}[\max(0, l_{SE} - l_{SE\_0})]^2 \quad (A10)$$

k_{SE} was chosen such that at F_{MAX} *SE* is at 104% of l_{SE_0}. For a graphical representation of the force–length relationships of the elastic components see Fig. A2, *A* and *B*. The muscle parameters, F_{MAX}, l_{SE_0}, and l_{CE_opt} were obtained from the literature (Murray et al. 1995, 2000; Nijhof and Kouwenhoven 2000; Kistemaker et al., unpublished observations). F_{SE} and F_{PE} were calculated using the muscle tendon complex length (l_{MTC}) and l_{CE}. Parameter values are listed in Table A2.

l_{MTC} was modeled as a second-order polynomial depending on elbow (φ_e) and shoulder angle (φ_s)

$$l_{MTC}(\varphi_e, \varphi_s) = a_0 + a_{1e}\varphi_e + a_{2e}\varphi_e^2 + a_{1s}\varphi_s \quad (A11)$$

a_{1e}, a_{2e}, and a_{1s} were based on cadaver data (Murray et al. 1995; Nijhof and Kouwenhoven 2000) obtained using the tendon displacement method (Grieve et al. 1978), values for a_0 representing l_{MTC} at $\varphi_e = \varphi_s = 0$ (and *width*, see *Eq. A8*) were chosen such that the optimum angle for maximal isometric moment was consistent with the literature (Chang et al. 1999; Kullig et al. 1984; Singh and Karpovitch 1968; Van Zuylen et al. 1988; Kistemaker et al., unpublished observations). Moment arms were calculated by taking the partial derivative of l_{MTC} to φ_e and φ_s

$$arm_e(\varphi_e) = \frac{\partial l_{MTC}}{\partial \varphi_e} = a_{1e} + 2a_{2e}\varphi_e \quad (A12)$$

$$arm_s(\varphi_s) = \frac{\partial l_{MTC}}{\partial \varphi_s} = a_{1s} \quad (A13)$$

APPENDIX B

Additional simulations to explore the effect of parameter values on model performance. To explore the sensitivity of the simulation outcome to changes in model parameters, additional simulations were carried out. Because it was previously shown that the model was capable of reproducing the salient static properties of the musculoskeletal system (Kistemaker et al. 2005; Kistemaker et al., unpublished observations), we focused on the model parameters determining the dynamic properties of the modeled muscles. The following parameters were varied one by one: m (increased by 10%; see *Eq. A1*), a_{rel} (increased by 10%; see *Eq. A5*), and b_{rel} (decreased by 10%; see *Eqs. A5* and *A6*). For each new parameter setting, the feedback gains were reoptimized and a simulation using the intermittent hybrid EP controller for the condition Flex1–3 was carried out. It was found that the changes in these parameters led to a small increase in RMS values (from 2.2 to 2.5, 2.6, and 2.8°, respectively), but that $\dot{\varphi}_p$ and t_{mov} were not significantly different from those observed experimentally (see Table B1). These results showed that the outcome of the present study was relatively insensitive to changes in parameters affecting the dynamical properties of the used muscle model.

The feedback gains found during the optimization process depended on the dynamics of the musculoskeletal system. This led to the question how sensitive the simulation outcome was to both changes in the dynamics of the system (e.g., inertia of the arm) and the feedback gains themselves. We performed simulations with 10% increased inertia, without reoptimizing the feedback gains, and we also performed simulations with feedback gains 10% lower than optimal. It was found that the performance of the model was not noticeably different: $\dot{\varphi}_{\max}$ and t_{mov} were not significantly different from those observed experimentally, whereas the RMS values were 2.4 and 2.3, respectively. This implies that for small changes in inertia, no adjustment of the feedback gains was needed and that the controller was robust for small errors in the feedback gains used.

In the INTRODUCTION it was stated that most EP controllers considered to date neglected tendon compliance and that joint angle was usually controlled by setting the appropriate muscle length using feedback from muscle spindles. However, muscle spindle feedback is related to muscle fiber length, whose relation to joint angle depends on force because of tendon compliance. To investigate the importance of taking tendon compliance into account, we investigated the static errors that occurred when the hybrid EP controller did not take the tendon compliance of the musculoskeletal model into account. The static error was found to depend on joint angle and cocontraction level and could be as large as 8°. Because humans are normally capable of controlling posture with much smaller error margins (also at maximal

TABLE A2. *Muscle specific parameters*

Muscle	F_{MAX}, [N]	l_{CE_opt}, [m]	l_{SE_0}, [m]	l_{PE_0}, [m]	a_0, [m]	a_{1e}, [m]	a_{1s}, [m]	a_{2e}, [m]
MEF	1420	0.092	0.172	0.129	0.286	−0.014	0	−3.96e-3
MEE	1550	0.093	0.187	0.130	0.236	0.025	0	−2.16e-3
BEF	414	0.137	0.204	0.192	0.333	−0.016	−0.030	−5.73e-3
BEE	603	0.127	0.217	0.178	0.299	0.030	0.030	−3.18e-3

MEF, monoarticular elbow flexor; BEE, biarticular elbow extensor.

TABLE B1. *Sensitivity of simulation results to changes in model and control parameters*

	$\dot{\varphi}_p$, deg s^{-1}	t_{pv}, s	t_{mov}, s	RMS, deg
h^m	984*	0.54	0.119*	2.5
h^{arel}	985*	0.52	0.120*	2.6
h^{brel}	981*	0.54	0.121*	2.8
h^J	977*	0.56	0.122*	2.3
h^{fb}	972*	0.55	0.121*	2.4
λ^+	783	0.89	0.145	20.5
h^δ	984*	0.49	0.120*	3.0
h^g	979*	0.64	0.119*	2.1
λ^{100ms}	811	0.91	0.150	11.2
λ^{+100ms}	993*	0.69	0.108	15.9
h^{100ms}	967*	0.60	0.111	3.9
h^{rc}	987*	0.57	0.120*	2.4
h^{10}	984*	0.57	0.120*	2.2
h^{15}	986*	0.59	0.119*	2.3
h^{20}	964*	0.54	0.121*	2.5
h^{50}	941	0.58	0.129	2.9
h^{250}	931	0.54	0.130	3.7
h^{1000}	932	0.55	0.130	3.6
h^i	986*	0.54	0.118*	2.3

All simulations for sensitivity analyses were done for one condition (Flex1–3). Note that the feedback gains were reoptimized for single movement using a minimal jerk trajectory (except for h^i). h^m, intermittent hybrid EP controller with slower activation dynamics ($m = 12.43$; see *Eq. A1*); h^{arel}, intermittent hybrid EP controller with slower contraction dynamics ($a_{rel} = 0.45$; see *Eq. A5*); h^{brel}, intermittent hybrid EP controller with slower contraction dynamics ($b_{rel} = 4.68$; see *Eqs. A5* and *A6*); h^J, intermittent hybrid EP controller with 10% increase in inertia of the lower arm plus hand; h^{fb}, intermittent hybrid EP controller with optimal feedback constants decreased by 10%; λ^+, λ-controller with reference velocity; h^δ, intermittent hybrid EP controller with increased feedback delay ($\delta = 0.3$; see *Eqs. 2* and *3*); h^g, intermittent EP controller with "gated" feedback such that feedback is absent at movements onset and offset; λ^{100ms}, intermittent λ-controller with duration of EP trajectory half the desired duration; λ^{+100ms}, intermittent λ-controller with reference velocity and duration of EP trajectory half the desired duration; h^{100ms}, continuous hybrid EP controller with duration of EP trajectory half the desired duration; h^r, intermittent hybrid EP controller with exponential reduced cocontraction 0.35 s after movement onset (see Fig. B1); $h^{15–1,000}$, intermittent EP controller at frequencies of 10, 15, 20, 50, 250, and 1,000 Hz; h^i, intermittent EP controller with feedback gains optimized for all six conditions using experimental data.

cocontraction level), this result suggested that EP controllers should take tendon compliance into account.

McIntyre and Bizzi (1993) suggested that the addition of a reference velocity in the feedback loop could increase movement speed. This leads to the question whether this could make the intermittent λ-controller produce movements as fast as those observed experimentally, as well as to the question whether the intermittent hybrid EP controller could still make movements as fast as those observed experimentally when the reference velocity was removed (i.e., set to zero). Additional simulations with the intermittent λ-controller showed that $\dot{\varphi}_p$ indeed increased (from 688 to 783°/s), but insufficiently to match that observed experimentally ($P < 0.001$) and at the cost of severe endpoint oscillations. As a result of those oscillations, the correspondence between simulated and experimentally observed kinematics was poor (RMS value of 20.5°; see Table B1), from which it was concluded that incorporating a reference velocity in the implemented intermittent λ-controller is not sufficient to make it suitable for the control of fast movements. Simulations with the intermittent hybrid EP controller showed that $\dot{\varphi}_p$ (mean value of 942°/s) was significantly lower ($P = 0.034$) than that observed experimentally when the reference contraction velocity was set to zero, and that RMS values increased to 3.4°. These results indicated that for the intermittent hybrid EP controller a reference velocity signal was needed to closely match the experimental data.

Feedback time delay diminishes the usefulness of feedback. To assess the influence of the delay on the present results, we also tested the model performance when δ was increased by 20%. Simulations showed that a longer delay gave rise to an increase in the RMS value (from 2.2 to 3.0°), but that neither $\dot{\varphi}_p$ nor t_{mov} was significantly different from values observed experimentally (see Table B1). This demonstrates that the hybrid EP controller would be capable of reproducing the experimentally observed data when longer latencies in the feedback loop are adopted.

Several experimental studies indicated that feedback is inhibited at movement onset and termination (e.g., Shapiro et al. 2002, 2004). We tested the performance of the hybrid EP controller when feedback was gated such that it was absent at movement onset and offset. This was implemented by multiplying the feedback components with a Gaussian function

$$STIM_h = \{STIM_{open} + (k_p[\lambda - l_{CE}(t - \delta)] + k_d[\dot{\lambda} - v_{CE}(t - \delta)])e^{-(t-t_p)^2/2\sigma^2}\}_0^1 \quad (B1)$$

Parameter t_p determines when this function attains its peak and parameter σ determines its width. Parameter t_p was set to 0.140 s and σ was set rather arbitrarily to 0.04 such that the Gaussian function was almost zero (0.002) at the start of the simulation. The results of the simulation showed that feedback gating did not distort the performance of the controller. $\dot{\varphi}_p$ still matched the experimentally observed peak angular velocity and the RMS value even decreased slightly to 2.1°. The diminished contribution of the feedback at movement onset was compensated by higher feedback gains. Because feedback was absent at movement onset and offset, the high feedback gains did not result in instability or oscillatory behavior. This result indicates that for the hybrid EP controller the presence of feedback at movement onset and offset is not necessary for adequately controlling fast point-to-point movements.

St-Onge et al. (1997) suggested that the duration of the EP trajectory underlying the control of fast movements was about the half of the duration intended (see also Ghafouri and Feldman 2001). It was investigated whether such a time-compressed EP trajectory improved the performance of the λ- and hybrid EP controllers. The simulations showed that the performance of the intermittent λ-controller improved, but not enough to match that of the subjects: $\dot{\varphi}_p$ was significantly lower than that observed experimentally ($P < 0.001$) and the RMS value was rather high (11.2°; see Table B1). Thus halving the duration of the EP trajectory did not allow the λ-controller to reproduce experimentally observed data. With such an EP trajectory the continuous hybrid EP controller reacted faster and reached a peak velocity (967°/s) that was not significantly different from the experimentally observed value (see Table B1). However, the RMS value was larger than that when the same controller was used with a normal EP trajectory (for which feedback gains were optimized for two conditions; see Table 2) and was almost twice as large as that of the intermittent hybrid EP controller with a normal EP trajectory (see Table B1). The reason was that the musculoskeletal model was not able to keep up with the time-compressed EP trajectory. Consequently, from the instant that the EP trajectory "reached" its endpoint and the reference velocity was set to zero, damping arising from feedback counteracted the movement. Clearly, an EP trajectory that "reaches" the endpoint long before the actual limb does (St-Onge et al. 1997) is not necessarily beneficial for the control of fast movements.

In this study, we used a cocontraction level that remained relatively high (yielding maximal stiffness) even when the final position was reached. Yet, EMGs of subjects show a gradual decrease near the end of the movement (see Figs. 4 and 5). To investigate whether a high level of cocontraction near the end of the movements was required to suppress overshoot or oscillations, simulations were carried out with the hybrid EP controller in which $STIM_{open}$ (and accompanying λ and $\dot{\lambda}$) was exponentially reduced toward the lowest possible $STIM_{open}$ that defined a stable EP at the final position. The exponential functions

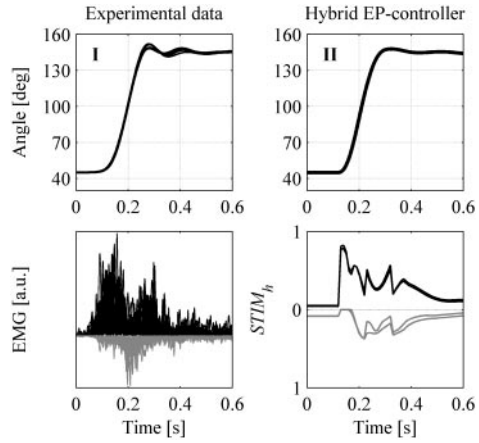

FIG. B1. Experimental data (*column I*, see also Fig. 4*A*) and simulation results obtained with the intermittent hybrid EP controller (*column II*). After the final position of the model had been reached, $STIM_{open}$ was exponentially reduced toward the lowest possible stimulation that defined an EP at this final position (λ and $\dot{\lambda}$ were changed accordingly). *Top EMG/$STIM_h$ traces* refer to the 2 elbow flexors, *bottom traces* to the 2 elbow extensors.

were applied 0.35 s after movement onset and contained a time constant of 0.080 s. The results of these simulations showed that the high level of cocontraction was not required to suppress the oscillations near the end of the movement (see Fig. B1). Obviously, peak angular velocity was not affected as the movement attained its peak velocity well before $STIM_{open}$ was diminished (see Table B1).

Experimental studies provided evidence that humans control their movements intermittently at frequencies in the range from 6 to 14 Hz. To test the sensitivity of the EP controller for the update frequency, we carried out additional simulations using a range of frequencies. When the update frequency was increased from 10 to 15 Hz, performance of the model did not change noticeably. However, simulations with update frequencies >20 Hz did not produce movements that matched those observed experimentally (see Table B1). Thus for the range of frequencies reported in the literature, the intermittent EP controller would be capable of reproducing the experimentally observed data.

Finally, we used a minimal jerk trajectory in the optimization process of the feedback gains, based on the rationale that the endpoint oscillations are not part of the desired trajectory (see METHODS). However, one might argue that even though the endpoint oscillations are not part of the desired trajectory, feedback gains should be optimized to reproduce features of experimentally observed movements. We investigated this option by reoptimizing the feedback gains for the hybrid EP controller for all six conditions using the trajectory including endpoint oscillations, and found that the RMS values decreased only slightly [in the case of condition Flex 1–3: from the RMS value of 2.5 (see Table 3) to 2.3]. Because valid arguments can be given for both optimization options, it is reassuring that they yielded comparable results.

In sum, the additional simulations showed that the outcome of this study did not critically depend on the values used for the model parameters.

APPENDIX C: GLOSSARY

$STIM_{closed}$	
EP	equilibrium point
Flex1–3	flexion movement from 50 to 150°
Ext2–1	extension movement from 100 to 50°
EMG	electromyography
φ_e	elbow angle
φ_s	shoulder angle
CE	contractile element
SE	series elastic element
PE	parallel elastic element
STIM	relative stimulation rate
$STIM_{open}$	open-loop muscle stimulation
$STIM_{closed}$	closed-loop muscle stimulation
$STIM_\alpha$	total *STIM* generated by α-controller
$STIM_\lambda$	total *STIM* generated by λ-controller
$STIM_h$	total *STIM* generated by hybrid EP controller
l_{CE}	*CE* length
λ	desired l_{CE}
l_{CE_opt}	*CE* optimum length
l_{CE_rel}	l_{CE}/l_{CE_opt}
v_{CE}	*CE* contraction velocity
λ	desired v_{CE}
l_{PE}	*PE* length
l_{PE_0}	*PE* slack length
l_{SE}	*SE* length
l_{SE_0}	*SE* slack length
k_p	l_{CE} feedback constant
k_d	v_{CE} feedback constant
δ	short-latency feedback delay
$\dot{\varphi}_p$	peak angular velocity
t_{pv}	time to peak velocity
t_{mov}	movement duration
l_{MTC}	muscle–tendon complex length
q	active state
γ_{rel}	relative amount of Ca^{2+}
F_{isom}	isometric force
F_{CE}	force delivered by *CE*
F_{MAX}	maximum isometric force
F_{SE}	force delivered by *SE*
F_{PE}	force delivered by *PE*

REFERENCES

Bellomo A and Inbar G. Examination of the gamma equilibrium point hypothesis when applied to single degree of freedom movements performed with different inertial loads. *Biol Cybern* 76: 63–72, 1997.

Bizzi E and Abend W. Posture control and trajectory formation in single- and multi-joint arm movements. *Adv Neurol* 39: 31–45, 1983.

Bizzi E, Accornero N, Chapple W, and Hogan N. Posture control and trajectory formation during arm movement. *Neuroscience* 4: 2738–2744, 1984.

Bogert AJ and Gerritsen GC, and Cole GK. Human muscle modelling from a user's perspective. *J Electromyogr Kinesiol* 8: 119–124, 1998.

Brown IE and Loeb GE. A reductionist approach to creating and using neuromusculoskeletal models. In: *Neuro-Control of Posture and Movement*, edited by Winters J and Crago P. New York: Springer-Verlag, 2000, p. 148–163.

Bullock D and Grossberg S. Emergence of tri-phasic muscle activation from the nonlinear interactions of central and spinal neural network circuits. *Hum Mov Sci* 11: 157–167, 1992.

Chang Y, Su F, Wu H, and An K. Optimum length of muscle contraction. *Clin Biomech* 14: 537–542, 1999.

Conway BA, Biswas P, Halliday DM, Farmer SF, and Rosenberg JR. Task-dependent changes in rhythmic motor output during voluntary elbow movement in man. *J Physiol* 501: P48–P49, 1997.

Conway BA, Reid C, and Halliday DM. Low frequency corlico-muscular coherence during voluntary rapid movements of the wrist joint. *Brain Topogr* 16: 221–224, 2004.

Craik KJW. Theory of the operator in control systems: I. The operator as an engineering system. *Br J Psychol* 38: 56–61, 1947.

de Lussanet MH, Smeets JB, and Brenner E. Relative damping improves linear mass-spring models of goal-directed movements. *Hum Mov Sci* 21: 85–100, 2002.

Doeringer JA and Hogan N. Intermittency in preplanned elbow movements persists in the absence of visual feedback. *J Neurophysiol* 80: 1787–1799, 1998.

Ebashi S and Endo M. Calcium ion and muscular contraction. *Progr Biophys Mol Biol* 18: 125–138, 1968.

Evans CM and Baker SN. Task-dependent intermanual coupling of 8-Hz discontinuities during slow finger movements. *Eur J Neurosci* 18: 453–456, 2003.
Feldman AG. Once more on the equilibrium-point hypothesis (lambda model) for motor control. *J Mot Behav* 18: 17–54, 1986.
Feldman AG, Adamovich SV, Ostry DJ, and Flanagan JR. The origins of electromyograms—explanations based on the equilibrium point hypothesis. In: *Multiple Muscle Systems: Biomechanics and Movement Organization*, edited by Winters JM and Woo SL-Y. London: Springer-Verlag, 1990, p. 195–213.
Feldman AG and Levin MF. The origin and use of positional frames of reference in motor control. *Behav Brain Sci* 18: 723–744,1995.
Funase K and Miles TS. Observations on the variability of the H reflex in human soleus. *Muscle Nerve* 22: 341–346, 1999.
Ghafouri M and Feldman AG. The timing of control signals underlying fast point-to-point arm movements. *Exp Brain Res* 137: 411–423, 2001.
Golub GH and Van Loan CF. *Matrix Computations*. Baltimore, MD: Johns Hopkins Univ. Press, 1989, p. 557–558.
Gomi H and Kawato. Equilibrium-point control hypothesis examined by measured arm stiffness during multijoint movement. *Science* 272: 117–120, 1996.
Gomi H and Kawato M. Human arm stiffness and equilibrium-point trajectory during multi-joint movement. *Biol Cybern* 76: 163–171, 1997.
Gottlieb GL. Muscle activation patterns during two types of voluntary single-joint movement. *J Neurophysiol* 79: 1860–1867, 1998a.
Gottlieb GL. Rejecting the equilibrium-point hypothesis. *Motor Control* 2: 10–12, 1998b.
Gribble PL and Ostry DJ. Compensation for loads during arm movements using equilibrium-point control. *Exp Brain Res* 135: 474–482, 2000.
Gribble PL, Ostry DJ, Sanguineti V, and Laboissiere R. Are complex control signals required for human arm movement? *J Neurophysiol* 79: 1409–1424, 1998.
Grieve DW, Pheasant S, and Cavanagh PR. Prediction of gastrocnemius length from knee and ankle joint posture. In: *Biomechanics VI-A*, edited by Asmussen E and Jorgensen K. Baltimore, MD: University Park Press, 1978, p. 405–418.
Gross J, Timmermann L, Kujala J, Dirks M, Schmitz F, Salmelin R, and Schnitzler A. The neural basis of intermittent motor control in humans. *Proc Natl Acad Sci USA* 99: 2299–2302, 2002.
Hanneton S, Berthoz A, Droulez J, and Slotine JJ. Does the brain use sliding variables for the control of movements? *Biol Cybern* 77: 381–393, 1997.
Hatze H. *Myocybernetic Control Models of Skeletal Muscle*. Pretoria, South Africa: Univ. of South Africa, 1981, p. 31–42.
Hermens HJ, Freriks B, Merletti R, Stegeman D, Blok J, Rau G, Disselhorst-Klug C, and Hägg G. SENIAM. European recommendations for surface electromyography. *Roessingh Res Dev* 1999.
Hof AL. The force resulting from the action of mono- and biarticular muscles in a limb. *J Biomech* 34: 1085–1089, 2001.
Hogan N. An organizing principle for a class of voluntary movements. *Neuroscience* 4: 2745–2754, 1984.
Kakuda N, Nagaoka M, and Wessberg J. Common modulation of motor unit pairs during slow wrist movement in man. *J Physiol* 520: 929–940, 1999.
Katz B. The relation between force and speed in muscular contraction. *J Physiol* 96: 45–64, 1939.
Kistemaker DA, Van Soest AJ, and Bobbert MF. Length dependent [Ca^{2+}] sensitivity adds stiffness to the muscle. *J Biomech* 38: 1816–1821, 2005.
Kullig K, Andrews JG, and Hay JG. Human strength curves. *Exerc Sport Sci Rev* 12: 417–466, 1984.
Lagarias JC, Reeds JA, Wright MH, and Wright PE. Convergence properties of the Nelder–Mead simplex method in low dimensions. *SIAM J Optim* 9: 112–147, 1998.
Latash ML and Gottlieb GL. Reconstruction of shifting elbow joint compliant characteristics during fast and slow movements. *Neuroscience* 43: 697–712, 1991.
Levin MF and Feldman AG. The lambda model for motor control: More than meets the eye. *Behav Brain Sci* 18: 786–806, 1995.
McIntyre J, and Bizzi E. Servo Hypotheses for the Biological Control of Movement. *J Mot Behav* 25: 193–202, 1993.
Merton, PA. Speculations on the servo-control of movements. In: *The Spinal Cord*, edited by Wolstenhilme GEW. London: Churchill Livingstone, 1953, p. 105–142.
Miall RC, Weir DJ, and Stein JF. Intermittency in human manual tracking tasks. *J Mot Behav* 25: 53–63, 1993.
Milner TE. Contribution of geometry and joint stiffness to mechanical stability of the human arm. *Exp Brain Res* 143: 515–519, 2002.
Murray WM, Buchanan TS, and Delp SL. The isometric functional capacity of muscles that cross the elbow. *J Biomech* 33: 943–952, 2000.
Murray WM, Delp SL, and Buchanan TS. Variation of muscle moment arms with elbow and forearm position. *J Biomech* 28: 513–525, 1995.
Nakano E, Imamizu H, Osu R, Uno Y, Gomi H, Yoshioka T, and Kawato M. Quantitative examinations of internal representations for arm trajectory planning: minimum commanded torque change model. *J Neurophysiol* 81: 2140–2155, 1999.
Nijhof E and Kouwenhoven E. Simulation of multijoint arm movements In: *Biomechanics and Neural Control of Posture and Movement*, edited by Winters J and Grago P. New York: Springer-Verlag, 2000, p. 363–372.
Ostry DJ and Feldman AG. A critical evaluation of the force control hypothesis in motor control. *Exp Brain Res* 153: 275–288, 2003.
Petrofsky JS and Phillips CA. The influence of temperature initial length and electrical activity on the force–velocity relationship of the medial gastrocnemius muscle of the cat. *J Biomech* 14: 297–306, 1981.
Pollok B, Gross J, Muller K, Aschersleben G, and Schnitzler A. The cerebral oscillatory network associated with auditorily paced finger movements. *Neuroimage* 24: 646–655, 2005.
Popescu F, Hidler JM, and Rymer WZ. Elbow impedance during goal-directed movements. *Exp Brain Res* 52: 17–28, 2003.
Prodoehl J, Gottlieb GL, and Corcos DM. The neural control of single degree-of-freedom elbow movements. Effect of starting joint position. *Exp Brain Res* 153: 7–15, 2003.
Schaal S. Arm and hand movement control. In: *The Handbook of Brain Theory and Neural Networks* (2nd ed.), edited by Arbib MA. Cambridge, MA: MIT Press, 2002, p. 110–113.
Schweighofer N, Arbib MA, and Kawato M. Role of the cerebellum in reaching movements in humans. I. Distributed inverse dynamics control. *Eur J Neurosci* 10: 86–94, 1998.
Shapiro MB, Gottlieb GL, and Corcos DM. EMG responses to an unexpected load in fast movements are delayed with an increase in the expected movement time. *J Neurophysiol* 91: 2135–2147, 2004.
Shapiro MB, Gottlieb GL, Moore CG, and Corcos DM. Electromyographic responses to an unexpected load in fast voluntary movements: descending regulation of segmental reflexes. *J Neurophysiol* 88: 1059–1063, 2002.
Singh M and Karpovitch VK. Strength of forearm flexors and extensors in men and woman. *J Physiol* 25: 177–180, 1968.
Stern JT. Computer modelling of gross muscle dynamics. *J Biomech* 7: 411–428, 1974.
St-Onge N, Adamovich SV, and Feldman AG. Control processes underlying elbow flexion movements may be independent of kinematic and electromyographic patterns: experimental study and modelling. *Neuroscience* 79: 295–316, 1997.
Suzuki M, Shiller DM, Gribble PL, and Ostry DJ. Relationship between co-contraction, movement kinematics and phasic muscle activity in single-joint arm movement. *Exp Brain Res* 140: 171–181, 2001.
Vallbo AB. Discharge patterns in human muscle spindle afferents during isometric voluntary contractions. *Acta Physiol Scand* 80: 552–566, 1970.
Vallbo AB and Wessberg J. Organization of motor output in slow finger movements in man. *J Physiol* 469: 673–691, 1993.
Van Ingen Schenau GJ, Bobbert MF, and Rozendal RH. The unique action of bi-articular muscles in complex movements. *J Anat* 155: 1–5, 1987.
Van Soest AJ and Bobbert MF. The contribution of muscle properties in the control of explosive movements. *Biol Cybern* 69: 195–204, 1993.
Van Zuylen EJ, Van Velzen A, and Denier van der Gon JJ. A biomechanical model for flexion torques of human arm muscles as a function of elbow angle. *J Biomech* 21: 183–190, 1988.
Wachholder K and Altenburger H. Beiträge zur Physiologie der willkürlichen Bewegung. IX. Mitteilung. Fortlaufende Hin- und Herbewegungen. *Pfluegers Arch* 214: 625–664, 1926.
Wessberg J and Vallbo AB. Pulsatile motor output in human finger movements is not dependent on the stretch reflex. *J Physiol* 15: 895–908, 1996.
Windhorst U. Shaping static elbow torque-angle relationships by spinal cord circuits: a theoretical study. *Neuroscience* 59: 713–727, 1994.
Windhorst U. Levers to generate movement. *Behav Brain Sci* 18: 784–785, 1995.
Winters JM and Stark L. Analysis of fundamental human movement patterns through the use of in-depth antagonistic muscle models. *IEEE Trans Biomed Eng* 32: 826–839, 1985.
Yamazaki Y, Suzuki M, and Mano T. Control of rapid elbow extension movement. *Brain Res Bull* 30: 11–19, 1993.
Zajac FE. Muscle and tendon: properties, models, scaling, and application to biomechanics and motor control. *Crit Rev Biomed Eng* 17: 359–411, 1989.